RevMexAA (Serie de Conferencias), **13**, 98–102 (2002)

Emission Lines from Jet Flows (Isla Mujeres, Q.R., México, November 13-17, 2000)
Editors: W. J. Henney, W. Steffen, A. C. Raga, & L. Binette

MHD JETS IN INHOMOGENEOUS MEDIA

S. O'Sullivan[1] and T. Lery[2]

RESUMEN

Presentamos simulaciones de la propagación de jets moleculares no-adiabáticos en un medio ambiente inhomogéneo. Los jets tienen condiciones descritos por un modelo de jet MHD en el cual la forma de las líneas magnéticas se prescribe cerca de la fuente. Perfiles de densidad ambiental fueron elegidos para representar la zona de transición entre las regiones exteriores de una nube molecular y el medio interestelar. Escalamos las tasas de enfriamiento atómico y molecular a niveles apropriados para resolver todas las escalas espaciales apropriadas. Con la inclusión de variabilidad de la fuente, las simulaciones reproducen varias características observacionales de jets moleculares, entre ellas las cavidades moleculares. Adicionalmente, encontramos similitudes entre teoría y observación para la fracción de ionización a lo largo del jet. Encontramos que la extensión lateral de las superficies de trabajo internas son sensibles al medio ambiente. También presentamos resultados preliminares para un método de calcular mapas de emisión en líneas usando solamente variables fundamentales de estado que parecen reproducir la emisión filamentosa de Balmer en frentes de choque.

ABSTRACT

We present simulations of the propagation of non-adiabatic molecular jets into an inhomogeneous ambient medium. The jets have inflow conditions described by a MHD jet model where the shape of the magnetic field lines is prescribed near the source. Ambient density profiles are chosen to represent the transition zone between the outer regions of a molecular cloud and the ISM. We have scaled the atomic and molecular cooling rates to appropriate levels in order to properly resolve all length scales involved. With the inclusion of source variability, the simulations reproduce several observational features of molecular jets such as molecular cavities. Additionally, we find similarities between theory and observation for the ionization fraction along the jet. The lateral extent of the internal working surfaces is found to be sensitive to the environment. We also present preliminary results from a method of calculating emission line maps using only fundamental state variables that seems to reproduce the observed filamentary Balmer emission on shock fronts.

Key Words: **ISM: JETS AND OUTFLOWS — MAGNETOHYDRODYNAMICS — STARS: PRE-MAIN-SEQUENCE**

1. INTRODUCTION

Nascent stars are found in regions of dense, cool molecular gas. Observations have shown that the accretion phase, during which the star builds up its mass, is very often accompanied by the powerful ejection of prominent bipolar outflows corresponding to fast jets (Ray et al. 1996) and molecular outflows (Bachiller 1996). There is strong evidence that these outflows interact dynamically with the ambient gas. In particular, integration of the momentum flux for HH jets over estimated lifetimes suggests that jets have sufficient momentum to drive their CO outflow counterparts (e.g., Mitchell et al. 1994). The proximity of H_2 bow shocks with enhanced CO emission (e.g., Davis & Eislöffel 1995) and SiO shocks with CO cavities (e.g., Gueth, Guilloteau, & Bachiller 1998) support this picture. So, the passage of well collimated jets through molecular regions may be closely associated with molecular outflows and therefore might be used to infer information about the earliest stages of star formation.

The propagation of jets through inhomogeneous media has been simulated from a hydrodynamic perspective by earlier authors. In particular, de Gouveia Dal Pino (1999) has considered three-dimensional collisions of over-dense, radiatively cooling jets with dense, compact clouds and found that such events may drive momentum transfer and turbulent mixing. The behaviour of jets in stratified media has also received some attention (Hardee et al. 1992; de Gouveia Dal Pino, Birkinshaw, & Benz 1996; de Gouveia Dal Pino & Birkinshaw 1996) and more recently, Rossi et al. 2000 have simulated a radiative jet impacting on a dense cloud. All of these works have employed "top-hat" profiles for the inflow, with a velocity shear layer in the case of Rossi et al. 2000.

In the following sections we shall briefly discuss numerical methods and present solutions from simu-

[1]Dept. of Applied Mathematics, U. of Leeds, Leeds.
[2]Dublin Institute for Advanced Studies, Dublin.

Emission Lines from Jet Flows (Isla Mujeres, Q.R., México, November 13-17, 2000)
Editors: W. J. Henney, W. Steffen, A. C. Raga, & L. Binette

lations. In the final section we investigate a method for calculating the dominant optical red lines of the emission spectrum typically observed from Herbig-Haro (HH) jets (Hα, [S II] $\lambda\lambda$ 6716, 6731, [O I] λ 6300, [N II] λ 6583) from the thermal pressure, temperature, H density and H ionization fraction without the need for complex tracking and atomic transition physics routines within the code.

2. COMPUTATIONAL DETAILS

The code employed solves the usual equations of MHD with the inclusion of cooling due to radiation from atomic species of solar abundances, dissociation of H_2 and ionization/recombination of H. The most salient remaining features of the code are that it incorporates a non-linear Riemann solver to handle strong rarefactions and an entropy advection scheme which maintains a positive definite internal energy in regions of smooth flow. For further details the reader is referred to O'Sullivan & Ray (2000).

For computational purposes it is obviously convenient to measure lengths in units of the initial jet radius $R_{\rm j} = 5 \times 10^{15}$ cm. Our computational domain is then $0 \le r \le 6$, $0 \le z \le 40$, spanned by square cells of dimension $\Delta = 0.02$. Under the rather severe restriction of a fixed grid geometry (postponing treatment with adaptive mesh refinement to future studies), we cannot resolve all length scales under conditions representative of a typical HH jet system. In particular, by looking at freely propagating one-dimensional shocks we have established that the post-shock cooling lengths for the models presented here are of order $\delta = 0.002$ and given the added complexity of two-dimensional flow this value may vary widely between different parts of the jet. This raises a dilemma in that we must choose between neglecting the dynamical importance of the cooling processes or rescale them to allow the corresponding length scales to be properly resolved. We choose the latter, with a scaling factor of 0.02, since the aim of this work is to investigate a method of calculating emission spectra which relies on properly tracking thermal energy through shocks.

3. INFLOW MODEL

The inflow parameters we use are obtained from a semi-analytical model for magnetocentrifugal launching from a magnetized rotator (Lery et al. 1998; Lery et al. 1999; Lery & Frank 2000). The rotator is specified as a boundary condition of the model and in this case is chosen in a multicomponent form to represent a central object with uniform angular velocity connected to a Keplerian disk via a sub-Keplerian transition zone. We vary the input parameters for the model to obtain pulsing at the inflow aperture with a 30 yr period as illustrated in Figure 1.

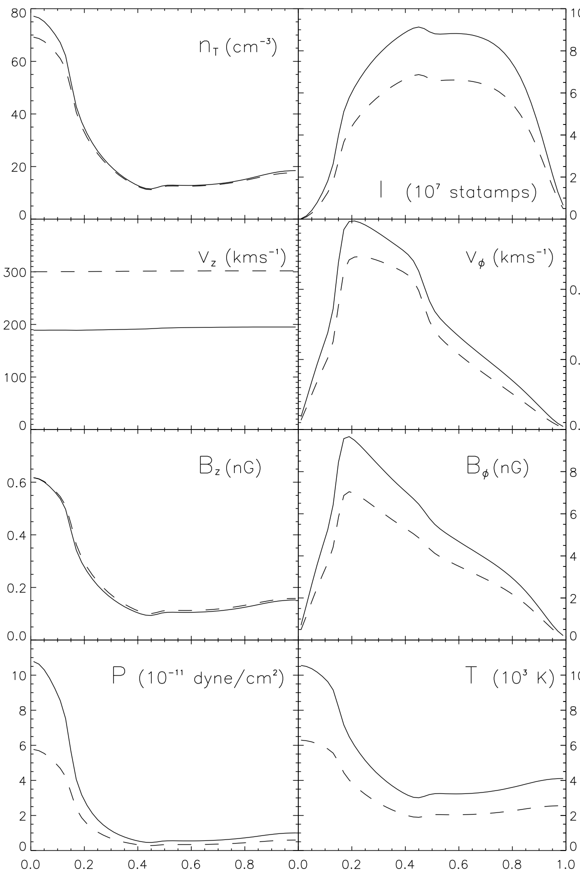

Fig. 1. Radial profiles of the nuclear number density, $n_{\rm T}$, total current, I, velocity, v, and magnetic field, B components, thermal pressure, and temperature. The half period (dashed line) and full period (solid line) profiles are shown.

For simplicity, the magnetic field included here is dynamically unimportant, even after non-adiabatic shock-driven compression, although there is no reason not to include strong fields in future work. Characteristic of this model it can be seen from Fig. 1 that the jet has a dense current carring core and a more tenuous collar carrying the return current. The molecular fraction of the jet is defined as $\eta^{\rm H} \equiv 2n^{\rm H_2}/n^{\rm H} = 0.1$ where $n^{\rm H_2}$ and $n^{\rm H}$ are the number densities of H and H_2. The axial velocity is essentially uniform across the jet and varies between 200 and 300 km s^{-1} over the injection cycle. It is also worth pointing out that the toroidal velocity component is non-zero and the jet is therefore transporting angular momentum from the source.

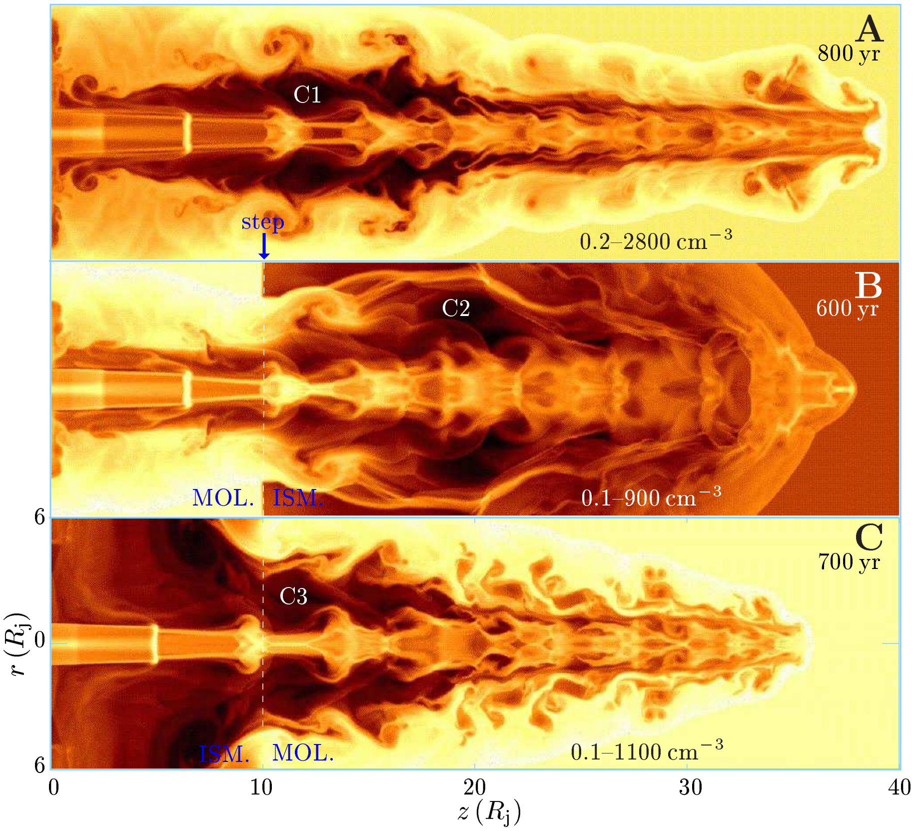

Fig. 2. Log-scale maps of the nuclear number density for three outflow models. Note the molecular cavities C1–C3 and the IWSs narrowing/widening as the jet propagates into high/low density material. NOTE: THIS FIGURE IS AVAILABLE IN COLOR IN THE ELECTRONIC VERSION OF THIS ARTICLE, OBTAINABLE FROM `http://www.astroscu.unam.mx/~rmaa/`.

4. SIMULATIONS

To investigate the behaviour of a jet near the edge of a molecular cloud we consider three models: (A) uniform molecular cloud (denoted MC henceforth); (B) step transition from MC to the ISM; (C) step transition to MC from ISM. For the discussion that follows we denote jet and ambient quantities with 'j' and 'a' subscripts. Further, we reference the core and collar of the jet with the subscripts 'cr' and 'cl' formally defining the core as the region $0 \leq r < R_{\rm c}$ and the collar as $R_{\rm c} \leq r \leq R_{\rm j}$ where $R_{\rm c}$ is the radius of minimum jet density. We also adopt the notation $\langle . \rangle$ to indicate a beam volume average at the input aperture. We have chosen ambient molecular conditions representative of the outer regions of a MC with temperature $T_{\rm a} = 100\,{\rm K}$, nuclear number density $n_{\rm a} = 200\,{\rm cm}^{-3}$ and molecular fraction $\eta^{\rm H} = 0.1$.

The ISM is set at $T_{\rm a} = 10^4\,{\rm K}$ and enforcing initial equilibrium with the molecular environment we obtain $n_{\rm a} = 1.9\,{\rm cm}^{-3}$ with $\eta^{\rm H} = 0$. The problem may then be parameterised in terms of the following dimensionless numbers with values for the molecular and ISM regions summarised in Table 1:

(i) $\eta^{\rm H}_{\rm j} \equiv (2n^{\rm H_2}/n^{\rm H})_{\rm j}$ and $\eta^{\rm H}_{\rm a} \equiv (2n^{\rm H_2}/n^{\rm H})_{\rm a}$, the jet and ambient molecular fractions;

(ii) $\langle \eta_{\rm cr} \rangle \equiv \langle n_{\rm cr} \rangle / n_{\rm a}$ and $\langle \eta_{\rm cl} \rangle \equiv \langle n_{\rm cl} \rangle / n_{\rm a}$, the ratios of the average nuclear number density in the core and collar of the jet to the ambient value;

TABLE 1

INITIAL PARAMETERS

Parameter	MC	ISM
$\eta^{\rm H}_{\rm a}$	0.1	0.0
$\langle \eta_{\rm cr} \rangle$	0.13	14
$\langle \eta_{\rm cl} \rangle$	0.08	8
$\langle \kappa_{\rm cr} \rangle$	8.2	8.2
$\langle \kappa_{\rm cl} \rangle$	2.7	2.7
$M_{\rm a}$	190–300	18–29

(iii) $\langle \kappa_{\rm cr} \rangle \equiv \langle P_{\rm cr} \rangle / P_{\rm a}$ and $\langle \kappa_{\rm cl} \rangle \equiv \langle P_{\rm cl} \rangle / P_{\rm a}$, the ratios of the average thermal pressure in the core and collar to the ambient value;

(iv) $\langle M_{\rm a} \rangle \equiv \langle v_{\rm j} \rangle / \langle c_{\rm a} \rangle$, the average Mach number with respect to the ambient material. Note that there are no magnetic parameters since the magnetic field is dynamically insignificant.

5. JET STRUCTURE

In Figure 2 we present log-scale plots of the H number density for the three outflow models under consideration. An interesting morphological fea-

Emission Lines from Jet Flows (Isla Mujeres, Q.R., México, November 13-17, 2000)
Editors: W. J. Henney, W. Steffen, A. C. Raga, & L. Binette

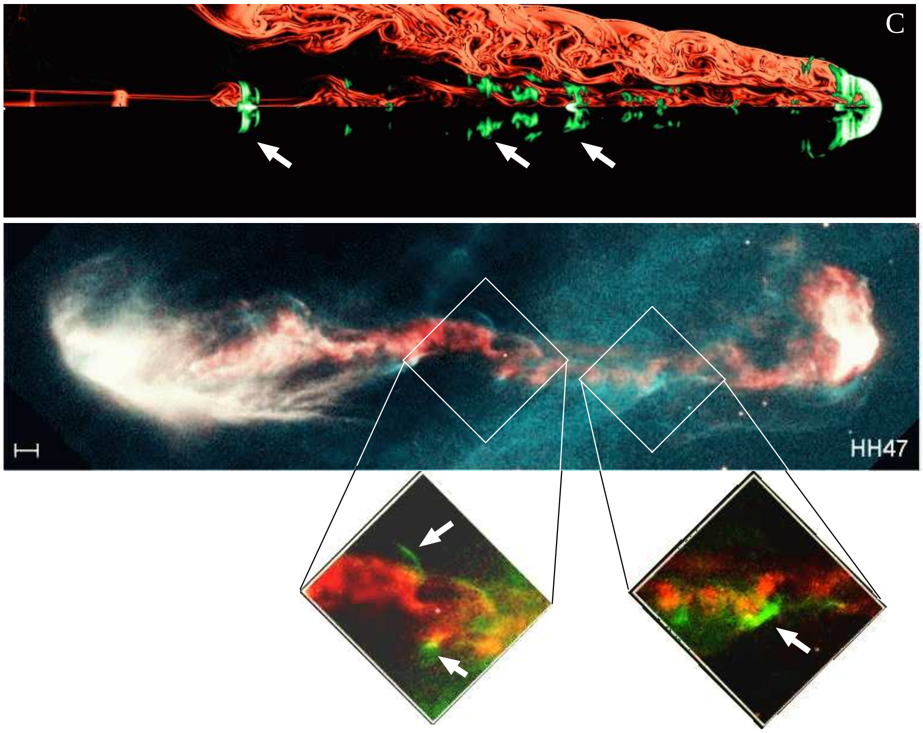

Fig. 4. Top: Convolved inverse colour map of Hα emission (blue) from Model C plotted with the density (orange) superposed above the axis. Bottom: *HST* composite picture of HH 47 in Hα (blue) and [S II] (red) (Credit: J. Morse/STScI, and NASA). Balmer filaments indicated by arrows in upper panel and lower panel insets. NOTE: THIS FIGURE IS AVAILABLE IN COLOR IN THE ELECTRONIC VERSION OF THIS ARTICLE, OBTAINABLE FROM `http://www.astroscu.unam.mx/~rmaa/`.

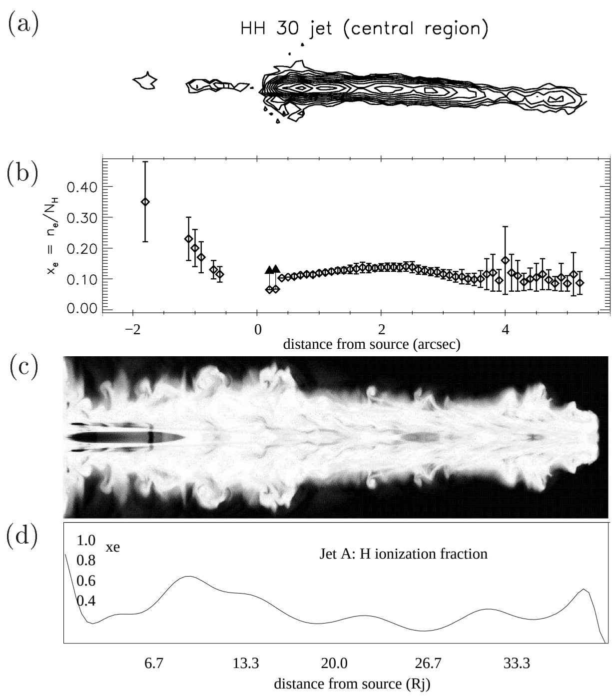

Fig. 3. (a) Contour plot of a [S II] *HST* image of the HH 30 jet. (b) Derived H ionization fraction x_{e} of HH 30 jet. (c) Logscale plot of Model A ionization fraction. (d) Bezier curve fit to Model A H ionization fraction x_{e} averaged in the direction transverse to the flow. (HH 30 panels adapted from Bacciotti et al. 1999)

ture of Model A, shown at 800 yr, is the molecular cavity cleared out by internal working surfaces (IWSs) which rapidly narrow as they travel along the beam. The structure here is reminiscent of cavities observed in such objects as the L 1157 molecular outflow (see, for example, Gueth et al. 1998). It should be noted here that our choice of inflow conditions for the jet will provide a far richer diversity of interactions within the extended structure of the jet than the conventional "top-hat" profiles more usually adopted. In particular, the core and collar of the jet have quite different density and pressure ratios with respect to the environment as elucidated by Table 1. If we look at the ionization fraction of H in Figure 3 it is evident that inflowing gas is rapidly ionized by crossing shocks and shows signs of recombination at later stages along the length of the beam. This is in some sort of qualitative agreement with values derived for HH 30 by Bacciotti, Eislöffel, & Ray (1999) as illustrated (the reader is also referred to the 2D maps the DG Tau jet (Bacciotti 2002) and the RW Aur jet (Dougados et al. 2002) presented at this conference). Both cases exhibit an overall "hump" in the ionization fraction moving away from the source. It should be pointed out that the simulated results for the ionization fraction in Fig. 3 are plotted over a range equivalent to twenty times that for the HH 30 data. This may be attributed, at least in part, to the scaling of the cooling processes.

The illustration of Model B in Figure 2 is our first result of a jet propagating through an inhomogeneous background. Although also containing an extended molecular cavity, its difference from Model A is immediately apparent. Once the jet pierces through the MC into the ISM, the beam material suffers a strong reflection shock on the axis and subsequently spreads into a dramatically inflating cocoon. The jet propagates more ballistically, reaching the edge of the computational domain after only 600 yr. These observations are not surprising, however, given that the jet is overpressured and making a transition between states of being underdense to overdense (see Table 1). The main bow shock has a rather more adiabatic form than would be expected if we had not rescaled the cooling processes thereby slowing the dissipation of thermal pressure support within the cocoon.

Model C is represented at 700 yr. In this case, since the jet is traveling from low to high density we see inverse effects to Model B: the IWSs begin to narrow as they enter the MC and the jet bow shock is far less extended. This suggests that the morphology of shocks may provide some sort of indicator as to the nature of the ambient environment.

6. EMISSION SPECTRA

Using a method inspired by Bacciotti (2002), we predict emission line intensities from the temperature, thermal pressure, atomic H density, and H ionization fraction of our simulated jets. At present, we may calculate emission maps in Hα, [S II] $\lambda\lambda$ 6716, 6731, [O I] λ 6300, and [N II] λ 6583. This is done on a cell-by-cell basis and integrated along the line of sight to provide a 3D projection. Figure 4 (see plate) shows the Hα emission from Model C plotted with the density superposed above the axis in comparison with a *HST* colour composite picture of HH 47. The map has been convolved to the approximate resolution of the *HST* image ($\sim 0''.05 \times 0''.05$). In both cases we can identify shocks through Hα Balmer emission (shown in insets). This occurs predominantly through collisional excitation in the thin heating zone at the front of the shock giving rise to the thin, wispy Balmer filaments along the leading edges of the internal working surfaces.

7. CONCLUSIONS

- Molecular cavities are reproduced effectively through the action of IWSs caused by variability at the source.
- We have found some qualitative agreement between observation and simulation of the ionization fraction along the jet beam.
- IWSs react to their environment becoming narrower in denser regions and vice-versa.
- We have presented preliminary results from a method for calculating emission line maps from fundamental state variables that reproduce filamentary Hα emission as observed in some HH jets.

The authors wish to thank F. Bacciotti for her contribution to the emission mapping and for much helpful discussion. We also thank A. Raga for the kernel of the emission code. We are grateful to the Dublin Institute for Advanced Studies for the use of its Beowulf cluster and to J. Walsh for maintaining it.

REFERENCES

Bacciotti, F. 2002, RevMexAA(SC), 13, 8 (this volume)
Bacciotti, F., Eislöffel, J., & Ray, T. P. 1999, A&A, 350, 917
Bachiller, R. 1996, ARA&A, 34, 111
Davis, C. J., & Eislöffel, J. 1995, A&A, 300, 851
de Gouveia Dal Pino, E. M. 1999, ApJ, 526, 862
de Gouveia Dal Pino, E. M., & Birkinshaw, M. 1996, ApJ, 471, 832
de Gouveia Dal Pino, E. M., Birkinshaw, M., & Benz, W. 1996, ApJ, 460, 111
Dougados, C., et al. 2002, RevMexAA(SC), 13, 43 (this volume)
Gueth, F., Guilloteau, S., & Bachiller, R. 1998, A&A, 333, 287
Hardee, P. E., White, R. E., III, Norman, M. L., Cooper, M. A., & Clarke, D. A. 1992, ApJ, 387, 460
Lery, T., & Frank, A., 2000, ApJ 533, 897
Lery, T., Heyvaerts, J., Appl, S., & Norman, C. A. 1998, A&A, 337, 603
__________. 1999, A&A, 347, 1055
Mitchell, G. F., Hasegawa, T. I., Dent, W. R. F., & Matthews, H. E. 1994, ApJ, 436, 177
O'Sullivan, S., & Ray, T. P. 2000, A&A, 363, 355
Ray, T. P., Mundt, R., Dyson, J. E., Falle, S. A. E. G., & Raga, A. C. 1996, ApJ, 468, 103
Rossi, P., Capetti, A., Bodo, G., Massaglia, S., & Ferrari, A. 2000 A&A, 356, 73

S. O'Sullivan: Department of Applied Mathematics, University of Leeds, Leeds LS2 9JT, UK (so@amsta.leeds.ac.uk).
T. Lery: Dublin Institute for Advanced Studies, 5 Merrion Square, Dublin 2, Ireland (lery@cp.dias.ie).